Damages induced by heavy ions in titanium silicon carbide: Effects of nuclear and electronic interactions at room temperature

J.C. Nappé [a,*], Ph. Grosseau [a], F. Audubert [b], B. Guilhot [c], M. Beauvy [b], M. Benabdesselam [d], I. Monnet [e]

[a] École Nationale Supérieure des Mines, SPIN/PMMC, LPMG UMR CNRS 5148, 158 cours Fauriel, 42023 Saint-Étienne cedex 2, France
[b] CEA, DEN, DEC/SPUA/LTEC, Cadarache, 13108 St Paul lez Durance, France
[c] École Nationale Supérieure des Mines, Centre CIS, 158 cours Fauriel, 42023 Saint-Étienne cedex 2, France
[d] Université de Nice - Sophia Antipolis, LPMC UMR CNRS 6622, Parc Valrose, 06108 Nice cedex 2, France
[e] GANIL/CIMAP/CIRIL, bd. Henri Becquerel, BP 55027, 14076 Caen cedex 5, France

ARTICLE INFO

ABSTRACT

Thanks to their refractoriness, carbides are sensed as fuel coating for the IVth generation of reactors. Among those studied, the Ti_3SiC_2 ternary compound can be distinguished for its noteworthy mechanical properties: the nanolamellar structure imparts to this material some softness as well as better toughness than other classical carbides such as SiC or TiC. However, under irradiation, its behaviour is still unknown. In order to understand this behaviour, specimens were irradiated with heavy ions of different energies, then characterised. The choice of energies used allowed separation of the effects of nuclear interactions from those of electronic ones.

© 2008 Elsevier B.V. All rights reserved.

1. Introduction

As part of Generation IV International Forum (GIF), new systems are studied, from the point of view of the reactor as well as the fuel cycle. These systems are characterised by an increased security level, better economic competitiveness, and an ability to recycle all the fuel in order to upgrade to a fissionable material and minimize long-lived waste production by transmutation. Among the six systems considered by the GIF, the Gas Fast Reactor (GFR) is studied in France; it is designed to work under helium-pressure and high-temperature (1100 – 1300 K).

These working conditions led to the selection of non-oxide refractory ceramics as fuel coating. Thus, carbides turn out to be great candidates thanks to their remarkable mechanical and thermal properties. However, their behaviour under irradiation has to be studied in more details.

Among the studied carbides, the ternary Ti_3SiC_2 presents some interesting prospects. Indeed, in 1972 Nickl et al. [1] remarked that this material, which was synthesized for the first time by a Viennese group in 1967 [2], is abnormally soft for a carbide. At the beginning of the 1990s, Pampuch et al. [3,4] and Lis et al. [5–7] led works on the pure bulk Ti_3SiC_2 synthesis; their best results were compounds with 80 – 90% purity, impurities being TiC_x and $TiSi_2$. During their works, they demonstrated that this material is both stiff (Young's modulus of 325 GPa) and soft (Vickers hardness of 6 GPa). Moreover, like Goto et al. [8] some years before, they noted that the hardness of this carbide decreases as the applied load increases; this property led them to qualify Ti_3SiC_2 as a 'ductile ceramic'.

At the end of the 1990s, Barsoum et al. [9–14] intensively studied this material as well as other ceramics with similar properties. In 2000 [15], they brought all these compounds together within one family of nanolamellar materials, named MAX Phases, of general formula $M_{n+1}AX_n$ where $n = \{1,2,3\}$, M is an early transition metal, A is an A-group (mostly IIIA and IVA) element, and X is C and/or N. Materials of this family are unusual in that they combine some properties of metals with those generally attributed to ceramics; thus, these materials are stiff, thermal and electrical conductors, readily machinable with tools for steels, and relatively soft and tough. More specifically, Ti_3SiC_2 is stable under inert atmosphere or vacuum up to 1975 K [9,13,16], resistant to quenching from 1475 K to room temperature [9,17], has a thermal conductivity of 37 $Wm^{-1} K^{-1}$ at room temperature and 32 $Wm^{-1} K^{-1}$ at 1775 K [13], a toughness of 9 MPa $m^{1/2}$ [15,18], a brittle – ductile mechanical transition as a function of temperature and strain rate [9,19–21], an electrical conductivity of $4.5 \times 10^6 \Omega^{-1}$ m^{-1} [9,15,22,23], and good corrosion resistance in common acids and NaOH (corrosion rate <300 μm a^{-1} in HNO_3, the worst case) [24–26]. Nevertheless, no information is available about its behaviour under irradiation.

Therefore, the aim of this study is a better knowledge of the behaviour under irradiation of Ti_3SiC_2, whose otherwise outstanding properties allow its consideration it as a cladding material for future fuels.

2. Experimental

The studied material is a polycrystalline commercial compound provided by 3-ONE-2 (Voorhees, NJ, USA). An estimation of the secondary phase proportion in the as-received material was carried out by X-ray Diffraction (XRD); the samples consist of about 80% Ti_3SiC_2, 15 % TiC_x, and 5 % $TiSi_2$. Fig. 1 shows the surface state of the as-polished specimens through Atomic Force Microscopy (AFM); the lower hardness of Ti_3SiC_2 compared with the TiC_x and $TiSi_2$ phases can be noted.

The as-received specimens were polished with diamond suspensions down to 1 μm. They were subsequently irradiated at room temperature with heavy ions. This kind of irradiation aims to simulate the interactions present in reactors (impacts of fission products, recoil atoms of alpha-decays, and neutrons) without the drawback of activating the specimens.

When heavy ions penetrate through a solid, they get decelerated via two different processes, namely, elastic collisions with target nuclei (with nuclear stopping power S_n) and inelastic collisions with target electrons (with electronic stopping power S_e). In order to understand the effects of both nuclear and electronic interactions on Ti_3SiC_2, two runs of irradiation were performed. The first one, called 'low energy irradiation', was achieved with the 4 MeV Au ions of the ARAMIS accelerator at the CSNSM of Orsay (France) to gain the nuclear interactions effects. The second one, named 'high energy irradiation', was made with the 90 MeV Xe ions delivered by the IRRSUD accelerator at the GANIL to understand the electronic interactions influence. Each run was carried out for 4

ion fluences: 10^{12}, 10^{13}, 10^{14} and 10^{15} cm^{-2}. The depths of the damaged zone were determined aided by the TRIM code [27].

To characterise surface modifications to the samples, two microscopic methods were used: Field Emission Gun Scanning Electron Microscopy (FEG-SEM) and AFM. The structure of the irradiated zone was analysed by Low Incidence XRD (LI-XRD) technique.

3. Results

The low energy irradiation spoils the first 500 nm of Ti_3SiC_2 essentially by nuclear interactions. By microscopic means, modifications are noticeable from a fluence of 10^{15} cm^{-2}. By FEG-SEM (Fig. 2), at some places it was noted that the Ti_3SiC_2 grain boundaries were eroded. This could be the consequence of preferential sputtering due to weaker displacement threshold energy of the atoms in grain boundaries than inside the grains. By AFM, surface etching can be observed; it may be explained by preferential sputtering as a function of the Ti_3SiC_2 crystallite orientation. In fact, orientation of the basal planes of the Ti_3SiC_2 hexagonal close-packed structure perpendicularly to the ion beam would lower the ion channeling effects inside the lattice, and so would increase the sputtering yield; therefore, as a function of the crystallite orientation, the sputtering yield would vary and so lead to this kind of microstructure. However, the as-irradiated surface is too spoiled to differentiate the three phases.

For the low energy irradiation, XRD was achieved under a 1° incidence angle (Fig. 3), which corresponds to a X-ray penetration of 230 nm in Ti_3SiC_2; Al peaks are from a mask intentionally laid on the virgin part of the samples during measurements. It brings out both a decrease of the peak intensity of the three phases as a
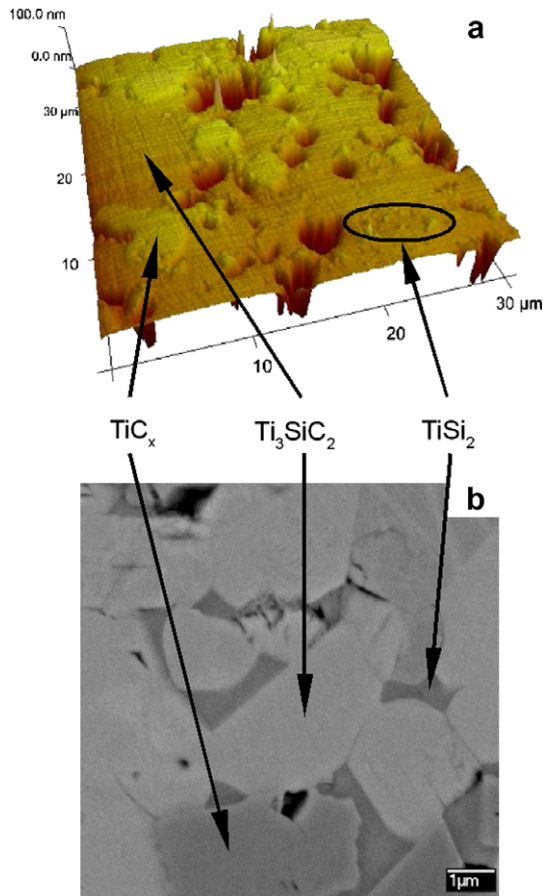
Fig. 1. Surface of as-polished Ti_3SiC_2 by AFM (a) and back-scattered electrons FEG-SEM (b)
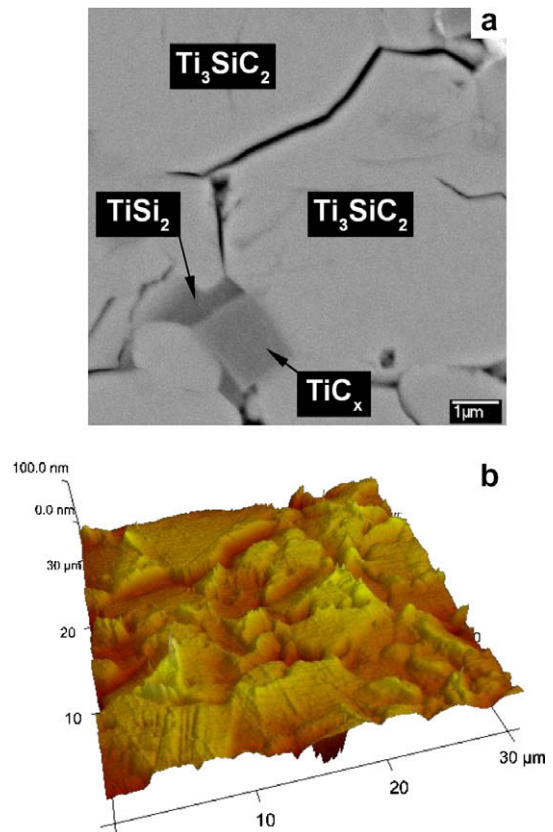
Fig. 2. Surface of Ti_3SiC_2 after Au (4 MeV) irradiation at a fluence of 10^{15} cm^{-2} by FEG-SEM (a) and AFM (b).
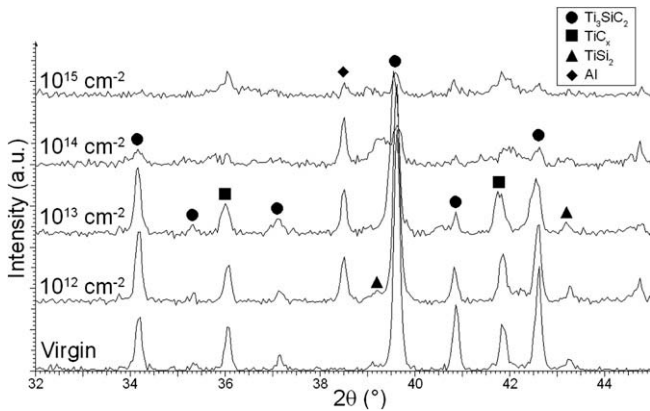
Fig. 3. XRD patterns of Au irradiated samples.

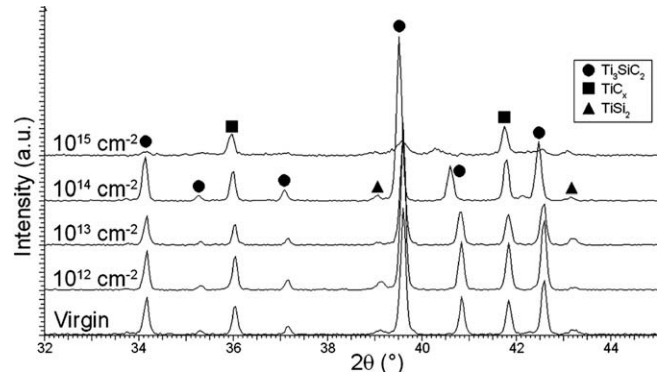**Fig. 5.** XRD patterns of Xe irradiated samples.

function of the Au fluence from 10^{14} cm^{-2}, and an increase of the baseline. These diffractogram changes are certainly due to a partial amorphisation of the material due to nuclear collisions. Indeed, this phenomenon was often encountered during irradiation of other materials such as SiC [28] or some oxides [29].

The high energy irradiation damages the first 5 μm of Ti$_3$SiC$_2$ by electronic interactions. Through FEG-SEM and AFM, two phenomena are revealed from Xe fluence of 10^{15} cm^{-2} fluence (Fig. 4):

– A surface etching due to different behaviour under irradiation of the phases present; the identification of the phases was performed by Energy Dispersive X-ray spectroscopy.
– The appearance of 'hills' on the Ti$_3$SiC$_2$ surface: their diameter varies from 50 to 100 nm, with a height of around 10 nm, and an estimated density of about $(1.0 – 1.5) \times 10^{10}$ cm^{-2}.
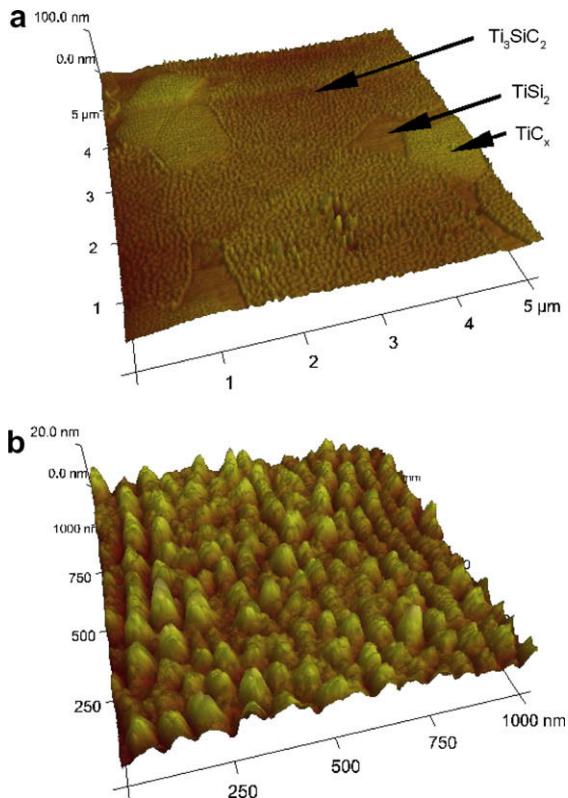

Fig. 4. Surface of Ti$_3$SiC$_2$ after Xe (90 MeV) irradiation at a fluence of 10^{15} cm^{-2} AFM; (a) 5×5 μm^2 scan and (b) 1×1 μm^2 scan of the Ti$_3$SiC$_2$ phase.

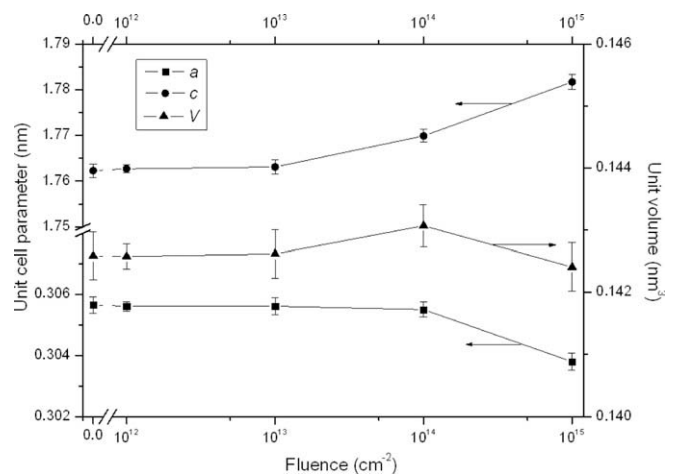**Fig. 6.** Ti$_3$SiC$_2$ unit cell parameters as a function of the Xe irradiation fluence; lines are only to guide the eye.

The XRD analysis was realised under a 3° incidence angle (Fig. 5), which corresponds to a X-ray penetration depth of 720 nm in Ti$_3$SiC$_2$. Diffraction patterns also reveal an amorphisation phenomenon, but only for Ti$_3$SiC$_2$ phase. Moreover, we can notice a modification of the unit cell of this compound; the peak initially located at 40.9°, relative to the (001) diffraction planes, is shifted to lower 2θ as a function of the fluence. Estimating the parameters of the unit cell as a function of the fluence (Fig. 6), an expansion of the unit cell along the c axis without significant variation of the unit volume may be underlined.

4. Discussion

Whereas the phenomena due to nuclear interactions can be understood through the elastic collisions during a low energy irradiation, those due to electronic interactions are often misunderstood. This discussion allows to brightening these phenomena.

The phenomenon of the appearance of 'hills' was apparently not yet observed in other materials for these conditions (energies of about 100 MeV and ion fluences close to 10^{15} cm^{-2}). Indeed, numerous authors remarked bumps during irradiations with similar energies, but generally fluences do not exceed some 10^{12} cm^{-2} [30–36]; thus they noted the same number of hills as of incident ions. In this case, authors usually attribute their appearance to the thermal spike model. The swift heavy ions lose energy during a short time ($<10^{-16}$ s) inside a cylindrical zone around the ion

trajectory. When S_e is higher than S_{eth} (threshold electronic stopping power) melting of the cylindrical zone followed by cooling and re-solidification lead to the formation of amorphous tracks inside the material. This phenomenon, which is more important at the near surface (where S_e is maximum), leads to high stresses and strains that would result in a flow of matter to form one hill by each ion. Only one paper notes about bumps for fluences higher than some 10^{12} cm^{-2} [34]; they noticed hills from lower fluence up to 2×10^{14} cm^{-2} and explained this by an agglomeration of the hills formed by thermal spikes. Nevertheless these explanations are not valid in our case: first, the density of hills is about 10^5 lower than the fluence, so thermal spikes cannot account for the bumps; second, this type of relief are only noted from 10^{15} cm^{-2} (not at lower fluences), so bumps are not due to agglomeration.

Other authors observed the same type of relief for very low energy ions (a few keV) at higher fluences (greater than 10^{16} cm^{-2}). In this case, the surface morphology would depend on both ion erosion and surface diffusion processes [37]. Other authors interpret this type of relief as the agglomeration of the projected ions at the very near surface of the target, implying the formation of nanobubbles [38] or nanoparticles [39]. Whatever the explanation, our fluences are too weak to allow the formation of 50 – 100 nm hills.

Defects noticed by LI-XRD are also not yet entirely understood. Amorphisation can be explained by several processes such as the formation of amorphous tracks by thermal spikes, irradiation induced microstrains in the unit cell, or a drop-off of the crystallite size. Irradiation induced microstrains seem to be an appropriate explanation since an expansion of the unit cell was also noted for Ti_3SiC_2.

In order to better understand these electronic interaction-induced phenomena, an in-depth study of the diffraction patterns is in progress. Observation of cross-sections by Transmission Electron Microscopy will also be performed.

5. Conclusion

This first study about damages induced by heavy ions in Ti_3SiC_2 at room temperature allows distinction between the effects of nuclear and electronic interactions on this remarkable ceramic. Elastic collisions lead to the amorphisation of all the phases of the specimens, sputtering of the Ti_3SiC_2 grain boundaries, and preferential sputtering as a function of the crystallite orientation. On the other hand, electronic interactions induce the amorphisation of only Ti_3SiC_2, expansion of the Ti_3SiC_2 unit cell along the c axis, and the formation of 'hills', the latter of which remains misunderstood yet.

Acknowledgment

References

[1] J.J. Nickl, K.K. Schweitzer, P. Luxenberg, J. Less-Common, Metals 26 (1972) 335.
[2] W. Jeitschko, H. Nowotny, Monatsh. Chem. 98 (1967) 329.
[3] R. Pampuch, J. Lis, L. Stobierski, M. Tymkiewicz, J. Eur. Ceram. Soc. 5 (1989) 283.
[4] R. Pampuch, J. Lis, J. Piekarczyk, L. Stobierski, J. Mater. Synth. Process. 1 (1993) 93.
[5] J. Lis, R. Pampuch, L. Stobierski, Int. J. Self-Propag. High-Temp. Synth. 1 (1992) 401.
[6] J. Lis, R. Pampuch, J. Piekarczyk, L. Stobierski, Ceram. Int. 19 (1993) 219.
[7] J. Lis, Y. Miyamoto, R. Pampuch, K. Tanihata, Mater. Lett. 22 (1995) 163.
[8] T. Goto, T. Hirai, Mater. Res. Bull. 22 (1987) 1195.
[9] M.W. Barsoum, T. El-Raghy, J. Am. Ceram. Soc. 79 (1996) 1953.
[10] M.W. Barsoum, T. El-Raghy, J. Mater. Synth. Process. 5 (1997) 197.
[11] M.W. Barsoum, T. El-Raghy, L. Ogbuji, J. Electrochem. Soc. 144 (1997) 2508.
[12] T. El-Raghy, A. Zavaliangos, M.W. Barsoum, S.R. Kalidindi, J. Am. Ceram. Soc. 80 (1997) 513–516.
[13] M.W. Barsoum, T. El-Raghy, C. Rawn, W.D. Porter, J. Phys. Chem. Solids 60 (1999) 429.
[14] M.W. Barsoum, T. El-Raghy, Metall. Mater. Trans. A 30 (1999) 363.
[15] M.W. Barsoum, Prog. Solid State Chem. 28 (2000) 201.
[16] R. Radhakrishnan, J.J. Williams, M. Akinc, J. Alloy. Compd. 285 (1999) 85.
[17] M.W. Barsoum, T. El-Raghy, Am. Scientist 89 (2001) 334.
[18] C.J. Gilbert, D.R. Bloyer, M.W. Barsoum, T. El-Raghy, A.P. Tomsia, R.O. Ritchie, Scr. Mater. 42 (2000) 761.
[19] M.W. Barsoum, M. Radovic, P. Finkel, T. El-Raghy, Appl. Phys. Lett. 79 (2001) 479.
[20] M. Radovic, M.W. Barsoum, T. El-Raghy, J. Seidensticker, S. Wiederhorn, Acta Mater. 48 (2000) 453.
[21] T. El-Raghy, M.W. Barsoum, A. Zavaliangos, S.R. Kalidindi, J. Am. Ceram. Soc. 82 (1999) 2855.
[22] N.F. Gao, Y. Miyamoto, D. Zhang, Mater. Lett. 55 (2002) 61.
[23] E.H. Kisi, J.A.A. Crossley, S. Myhra, M.W. Barsoum, J. Phys. Chem. Solids 59 (1998) 1437.
[24] V.D. Jovic, M.W. Barsoum, J. Electrochem. Soc. 151 (2004) B71.
[25] V.D. Jovic, B.M. Jovic, S. Gupta, T. El-Raghy, M.W. Barsoum, Corros. Sci. 48 (2006) 4274.
[26] J. Travaglini, M.W. Barsoum, V.D. Jovic, T. El-Raghy, Corros. Sci. 45 (2003) 1313.
[27] J.F. Ziegler, <www.srim.org/>.
[28] A. Audren, A. Benyagoub, L. Thomé, F. Garrido, Nucl. Instrum. Methods B 257 (2007) 227.
[29] M. Beauvy, C. Dalmasso, C. Thiriet-Dodane, D. Simeone, D. Gosset, Nucl. Instrum. Methods B 242 (2006) 557.
[30] K.R. Mavani, D.S. Rana, S. Rayaprol, R.N. Parmar, D.G. Kuberkar, R. Kumar, M. Tonouchi, J. John, R. Nagarajan, Solid State Commun. 142 (2007) 462.
[31] P.C. Srivastava, V. Ganesan, O.P. Sinha, Nucl. Instrum. Methods B 187 (2002) 220.
[32] V.A. Skuratov, D.L. Zagorski, A.E. Efimov, V.A. Kluev, Y.P. Toporov, B.V. Mchedlishvili, Radiat. Meas. 34 (2001) 571.
[33] V.A. Skuratov, A.E. Efimov, K. Havancsak, Nucl. Instrum. Methods B 250 (2006) 245.
[34] R.L. Dubey, S.K. Dubey, A.D. Yadav, S.J. Gupta, S.D. Pandey, T.K. Gundu Rao, T. Mohanty, D. Kanjilal, Nucl. Instrum. Methods B 257 (2007) 287.
[35] S. Ghosh, V. Ganesan, S.A. Khan, P. Ayyub, N. Kumar, Appl. Surf. Sci. 252 (2006) 8223.
[36] J.F. Carlotti, A.D. Touboul, M. Ramonda, M. Caussanel, C. Guasch, J. Bonnet, J. Gasiot, Appl. Phys. Lett. 88 (2006) 1.
[37] S. Rusponi, G. Costantini, C. Boragno, U. Valbusa, Phys. Rev. Lett. 81 (1998) 2735.
[38] Y. Yamauchi, T. Taguchi, Y. Hirohata, T. Hino, M. Nishikawa, Vacuum 74 (2004) 479.
[39] A.L. Stepanov, V.N. Popok, Surf. Sci. 566–568 (2004) 1250.